Hindawi
Geofluids
Volume 2022, Article ID 6564345, 10 pages
https://doi.org/10.1155/2022/6564345

Research Article

Unconfined Compression Test on In Situ Frozen Clay Sampled from Frozen Wellbore

Heng Wang,[1,2,3] **Gongzhou Li**,[4] **Fangbo Ning**,[2,3] **Wei Gao**,[2,3] **and Bin Su**[4]

[1]*Coal Research Institute, Beijing 100013, China*
[2]*National Engineering Research Center of Deep Shaft Construction, Beijing 100013, China*
[3]*Beijing China Coal Mine Engineering Co., Ltd., Beijing 100013, China*
[4]*China Electronics Engineering Design Institute Co., Ltd., Beijing 100142, China*

Correspondence should be addressed to Gongzhou Li; ligongzhou@263.net

Received 26 December 2021; Accepted 8 February 2022; Published 8 March 2022

Academic Editor: Dongdong Ma

Based on the current shortcomings in frozen wall designations, in which the unconfined compressive strength test parameters of undisturbed and remolded frozen soils are used for calculations, in situ frozen soil samples were taken from a frozen wellbore, and unconfined compressive strength tests were performed in this study. The test results showed significant discreteness in the in situ freezing uniaxial compressive strength of the cohesive soil, with low test repeatability. Because of the anisotropy of the original soil structure, the elastic modulus of 31.3% of the undisturbed frozen soil was found to be lower than that of the remolded frozen soil at the same temperature, and it was 0.5–2.1 times the elastic modulus of the remolded frozen soil. This value was negatively correlated with the freezing temperature; however, it had no evident relationship with the occurrence depth of the frozen soil. Based on the design principle of the frozen wall of the west air shaft in Zhaogu No. 2 Mine, the thickness calculated by substituting the in situ frozen soil test parameters was 1.14–1.61 times that of the original design of the frozen wall of the viscous soil layer.

1. Introduction

Frozen soil is a type of special rock/soil composed of four basic components: solid particles, ice, liquid water, and gas. It is heterogeneous and anisotropic. Its particularity is mainly manifested in two aspects: the temperature and cementation of the soil particles with ice. Frozen soil formed under natural low-temperature conditions can be broadly divided into short-term, seasonal, and perennial permafrost [1, 2].

The artificial ground freezing (AGF) method is a construction method developed on the basis of seasonal frozen soil. It was first used to prevent the collapse of shallow mine roofs and has gradually been applied to the construction process of shafts under special stratum conditions. Since the introduction of the AGF method in China in 1955, it has been used in construction for more than 60 years. As of 2016, more than 1200 shafts have been constructed using the AGF method. With the revisions made by China to its energy policy, the development of coal mines has gradually decreased, and the application of the AGF method has been extended to nonferrous metal mines, water conservancy projects, and municipal projects [3–6].

The water in the soil is distributed differently before and after the freezing of the soil because of the existence of potential energy, resulting in the migration of water in rock/soil. In other words, in a low-temperature environment, the temperature gradient drives pore water to migrate from the unfrozen area to the frozen front and condense into ice, and thus, the water in the soil undergoes redistribution [1, 3]. On the one hand, the ice lens formed destroys the original stable structure of the soil and deteriorates its mechanical properties. On the other hand, the cementation of the ice particles strengthens the ability of the soil skeleton to resist external loads, which indicates that frozen soil has a significantly higher strength than unfrozen soil.

Generally, the strength parameters of frozen soil are obtained by performing mechanical tests in a laboratory

with remolded soil. However, the undisturbed soil conditions and structural differences lead to a significant difference between the mechanical properties of undisturbed and remolded soils [7]. When the mechanical parameters of a remolded frozen soil are applied in the design of natural foundations or frozen walls in the original state, the calculation results are biased, and it should be modified in practical applications [8–10]. Experimental parameters can be obtained from undisturbed soil collected from a wellbore inspection hole [11–13]. A comparison between laboratory data of the mechanical properties of undisturbed and remolded soils has shown that the failure mechanism of undisturbed frozen clay is brittle failure (failure surface penetration, with a destruction angle of 31–44°), whereas that of remolded frozen clay is plastic failure ("drum" shaped, distribution of tiny cracks). However, the conservation of undisturbed frozen soil, which is obtained from the drilling hole, is a process of water migration at low temperatures under the condition of the original moisture content, and ice lenses are easily formed at the contact end of the cold source [14–18].

Currently, the existing frozen soil test is generally based on sampling from the wellbore inspection hole. In this case, the test results cannot fully reflect the real original characteristics of the frozen soil; a frozen soil "block" taken from inside the wellbore is in a good original state, and the migration and redistribution process of most of the free water would have been completed. The parameters obtained from the physical and mechanical tests have better guiding significance for freezing wall design and freezing control processes.

Frozen soil was sampled from inside a frozen shaft of Zhaogu No. 2 Mine, and an uniaxial test was conducted under an unconfined compression condition. The obtained parameters and those from the remolded soil experiment were compared and analyzed to determine the differences between them. Based on the test parameters, the thickness of the frozen wall of the west air shaft of Zhaogu No. 2 Mine was calculated. By comparing with the original design parameters, the influence degree of the different sampling methods on the design calculation results of the frozen wall thickness was analyzed.

2. Test Device and Process

In accordance with the "Test Method for Uniaxial Compressive Strength of Artificial Frozen Soil" (MT/T593.4-2011), frozen soil was sampled from the west air shaft of Zhaogu No. 2 Mine underground and then transported to a laboratory after on-site packaging. First, the actual water content and density were tested (Table 1 shows the results), and the samples were then prepared on the basis of the requirements of the unconfined compressive strength test, with the error requirements not exceeding ±1.0% and 0.3 g/cm^3.

The undisturbed soil test was conducted by cutting large undisturbed frozen soil blocks with sawing and lathe machines in a low-temperature environment. The sample size was $\phi 61.8 \times 150$ mm, and the magnitude of the error was kept within ±0.2%. After the undisturbed frozen soil tests, the samples were broken, dried at 105°C, and cooled. Water was then distributed based on the moisture content of the undisturbed soil, and the sample was then molded to a size of $\phi 61.8 \times 150$ mm.

Table 1: Sampling distribution and basic parameters of the frozen soil in Zhaogu No. 2 Mine.

No.	Lithology	Buried depth/m	Moisture content/%	Density g/cm^3
A1	Clay	430	13.60	2.16
A2	Sandy clay	485	11.35	2.19
A3	Clay	590	10.48	2.28
A4	Clay	650	13.95	2.16

The unconfined compressive strength test of the frozen soil samples was designed with four negative temperature grades: −10, −15, −20, and −25°C. During the specimen curing period, continuous cooling was provided to ensure that the ambient temperature of the specimen was maintained in the designed constant temperature level required by the frozen soil test; its fluctuation range was controlled within ±0.2°C.

For the unconfined compressive strength test of the frozen soil samples, a constant-strain rate control loading method was adopted with a strain rate of 1%/min [19–26]. An uniaxial compressive strength test was conducted on the frozen soil without confining pressure using WDT-100 frozen soil testing machine. Figures 1 and 2 show the testing machine and loading fixture, respectively.

The unconfined compressive strength of the frozen soil was tested in the undisturbed and remolded frozen states, with four layer tests (Table 1). At least three samples were taken for each temperature grade for parallel tests to improve the accuracy of the test results. A total of 100 samples were processed, including 52 undisturbed samples and 48 remolded samples.

3. Unconfined Compression Test Results and Analysis

3.1. Analyses of Uniaxial Compressive Strength, Elastic Modulus, and Poisson's Ratio. Table 2 presents the test results of the uniaxial compressive strength, elastic modulus, and Poisson's ratio of the frozen soil, obtained from unconfined compressive strength tests conducted on 100 samples (arithmetic mean values are taken). Figure 3 shows the curves.

In Figure 3, the uniaxial compressive strength of the undisturbed frozen soil and remolded frozen soil increases with the decrease in the temperature. Due to the influence of primary cracks in the frozen soil samples, the uniaxial compressive strength values of the undisturbed frozen soil at different temperatures are highly discrete, and the test repeatability is low. The test values of the uniaxial compressive strength of the artificially remolded frozen soil are highly concentrated and repeatable. The uniaxial compressive strength of the frozen soil under the same stratum

Figure 1: Unconfined compressive strength testing machine for frozen soil.

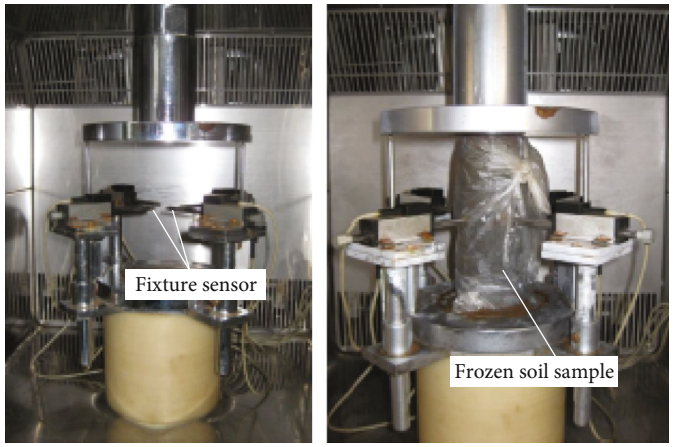

Figure 2: Unconfined compressive strength testing fixture for frozen soil.

condition with different temperatures can be estimated using the interpolation method.

3.1.1. Uniaxial Compressive Strength. Based on the test values of the undisturbed frozen soil in Table 2, the uniaxial compressive strength values of the undisturbed frozen soil at the same test temperature show the following rules:

-10°C: A3 > A2 > A1 > A4
-15°C: A2 > A1 > A3 > A4
-20°C: A2 > A1 > A3 > A4
-25°C: A1 > A2 > A4 > A3

The results show that under the condition of no confining pressure, the temperature of the undisturbed frozen soil and remolded frozen soil is negatively correlated with the uniaxial compressive strength, and the uniaxial compressive strength of the remolded frozen soil also shows similar properties. The results show that the uniaxial compressive strength of the frozen soil slightly increases when the water content and density are the same, and the stress of the original rock/soil is released. The two experimental values of the frozen soil indicate that the internal fissures in the undisturbed frozen soil have little effect on the change in the uniaxial compressive strength of the frozen soil.

3.1.2. Elastic Modulus of Frozen Soil. Under the condition of constant strain rate and no confining pressure, the elastic modulus of the undisturbed and remolded frozen soil increases with the decrease in the frozen soil temperature. This is because the compressive strength of the ice and soil particle bond increases at low temperature, and a greater stress value is required to maintain a constant strain rate. Meanwhile, there is a relatively concentrated and stable region in the elastic modulus–temperature curve in Figure 3, with the elastic modulus ranging from 200 MPa to 250 MPa, corresponding to a sample temperature of approximately 19°C. A further study is required to confirm the correlation and accuracy of the temperature and elastic modulus values in this region.

Table 2: Summary data of uniaxial test results of frozen soil.

No.	Temperature/°C	Uniaxial compressive strength/MPa		Elasticity modulus/MPa		Poisson's ratio	
		YZ	CS	YZ	CS	YZ	CS
A1	−10	3.73	3.66	87.8	97.62	0.36	0.34
	−15	5.56	4.63	197.37	156.56	0.34	0.3
	−20	6.43	5.95	208.32	175.05	0.41	0.31
	−25	8.78	7.23	193.6	298.01	0.41	0.28
A2	−10	4.19	2.9	175.04	147.51	0.39	0.3
	−15	6.91	4.37	314	114.24	0.38	0.25
	−20	7.24	5.53	558.2	239.93	0.33	0.26
	−25	8.39	6.54	568.78	317.48	0.32	0.22
A3	−10	4.63	2.41	209.96	119.69	0.41	0.46
	−15	4.41	4.01	206.3	173.48	0.37	0.41
	−20	5.75	4.51	218.59	170.11	0.34	0.41
	−25	6.86	5.23	235.71	143.29	0.42	0.3
A4	−10	1.8	3.12	90.2	116.4	0.33	0.39
	−15	3.42	4.39	102.3	236.4	0.2	0.38
	−20	5.04	5.3	250.25	206.44	0.32	0.32
	−25	7.41	7.05	323.45	243.36	0.43	0.44

*YZ: undistributed frozen soil; CS: remolded frozen soil.

3.1.3. Poisson's Ratio of Frozen Soil. The Poisson's ratio of the remolded frozen soil decreases with the decrease in the test temperature, and the variation trends in the Poisson's ratio of the four layers are completely consistent (except for A4 layer −25°C). However, the Poisson's ratio of the undisturbed frozen soil has significant dispersion and follows no specific law. The results show that the anisotropic structure of undisturbed frozen soil determines the ratio of vertical and radial deformation under no confining pressure. However, the ratio of the vertical and radial deformations of the remolded frozen soil samples is stable, and the uniformity inside the samples determines the variation difference in the vertical and radial deformations. Moreover, further studies are required to be able to apply the mechanical parameters obtained from the frozen soil test conducted on the remolded samples for freezing design.

3.2. Analysis of Stress–Strain Changes of Frozen Soil Samples. Figure 4 shows the stress–strain curves of the unconfined frozen soil and remolded frozen soil in the A2 layer under unconfined compression.

Figure 4 shows the stress–strain curves of A2 undisturbed frozen soil and remolded frozen soil without confining pressure. The stress–strain curves of the frozen soil without the confining pressure can be divided into four stages (Figure 4(c)): (1) OA, elastic deformation stage. The strain of the samples increases with the increase in the stress, and the relationship between them is approximately linear. It is a process in which the original microcracks in the undisturbed frozen soil are gradually compacted (the cracks in the remolded soil are generated during the manual compaction of the samples). (2) AB, elastic-plastic deformation stage. The strain increases more faster with the stress growth. In the process of gradual pressure increase, the frozen soil samples undergo a small fracture damage, and the fissures connect more rapidly. The ε value of the undisturbed soil, corresponding σ value, is significantly lower, which means the elastic modulus of the undisturbed soil is greater than the elastic modulus of the remolded soil. (3) BC, failure stage. In this stage, the stress value reaches the peak, and the specimen is damaged. (4) CD, postdestruction stage. The stress of the undisturbed frozen soil decreases rapidly in a short time because of the structural failure (X conjugate shear or splitting failure) but does not fall to 0, indicating that the undisturbed soil still has a certain bearing capacity after damage. This is because the undisturbed soil particles are uneven, and larger particles are formed naturally, or that the strength of the frozen ice is high. Due to the grinding and screening of the remolded soil, the soil particles are uniform and small; therefore, the test block is in a bulging state after destruction, and the stress and strain gently decrease.

Based on the stress–strain relationship curve slope shown in Figure 4, before the frozen soil sample destruction (the C point), the elastic modulus of the frozen soil in the original state is greater than that of the remolded frozen soil. However, from all the test data, the elastic modulus of the undistributed frozen soil is not greater than the remolded frozen soil elastic modulus, and its range of E (YZ) is (0.5–2.1) E (CS). The elastic modulus of 31.3% of the 100 samples is lower than that of the remolded frozen soil sample. This is because the anisotropy due to the characteristics of the primary joints and fissures in the undisturbed frozen soil lead to significant dispersion in the elastic modulus. At the same time, the failure time of the undisturbed frozen soil is inconsistent with the failure time of the remolded frozen soil. Therefore, the time effect of the stress–strain should be paid

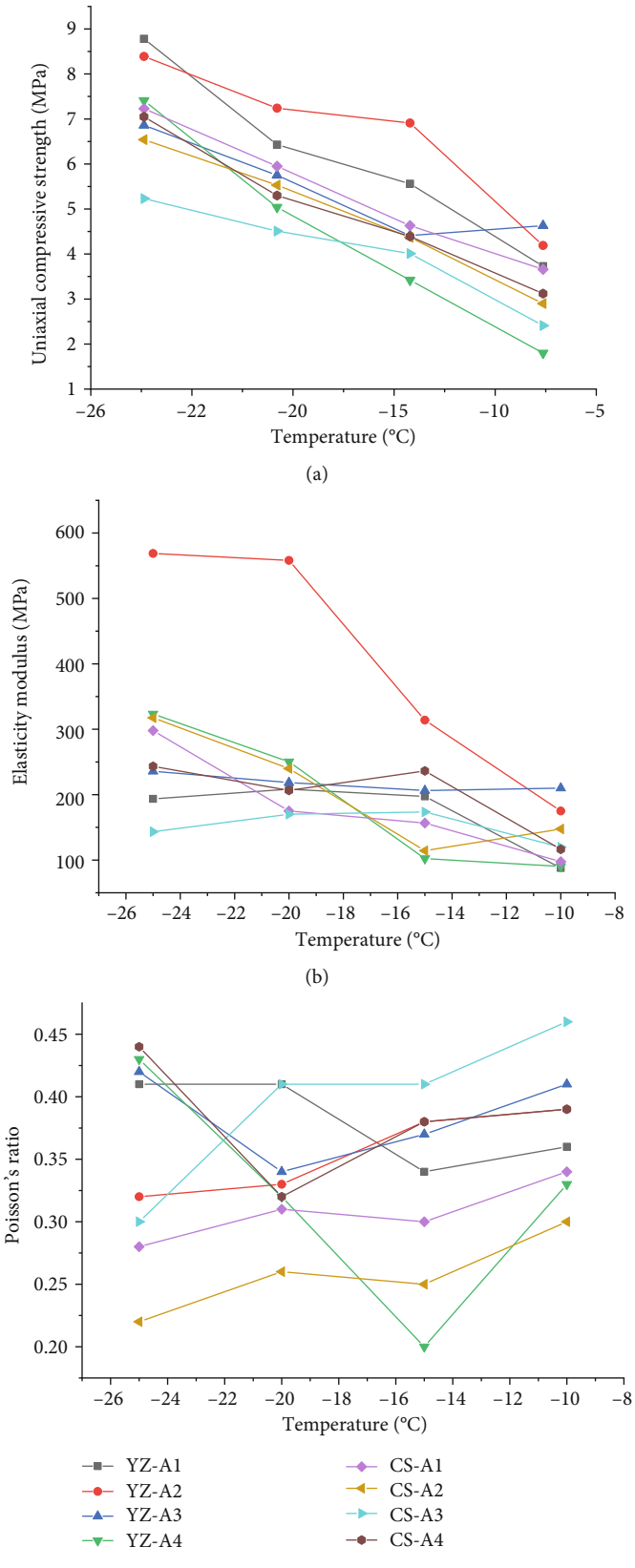

Figure 3: Variation curves of the (a) uniaxial compressive strength, (b) elastic modulus, and (c) Poisson's ratio of the undisturbed and remolded frozen soils at different temperatures.

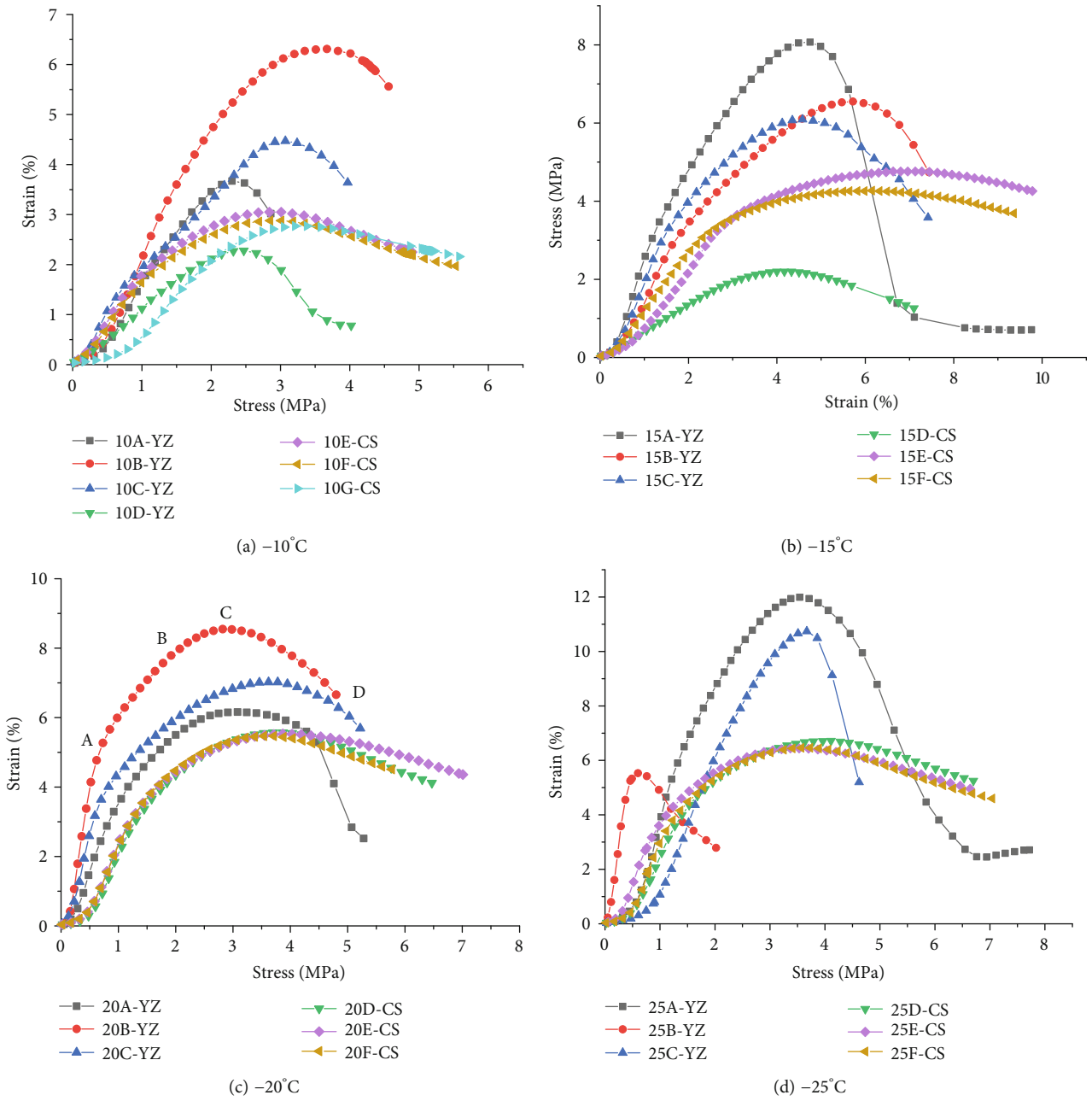

Figure 4: Stress–strain curves of the undisturbed permafrost and remolded permafrost in the A2 layer.

attention in the actual excavation stage of artificial frozen soils, and the displacement monitoring of the frozen wall is an important means to ensure the safety of shaft excavation.

4. Calculation of Frozen Wall Thickness

As an example, this study takes the frozen wall design of the west air shaft of Zhaogu No. 2 Mine from where frozen soil samples were collected. Based on the original frozen wall design scheme, the differences between the design and the original design in terms of the frozen wall thickness under the conditions of frozen soil parameters after water migration were determined.

4.1. Original Design of Frozen Wall Thickness of West Air Shaft of Zhaogu No. 2 Mine. The thickness of the alluvial layer in the west air shaft of Zhaogu No. 2 Mine is 704.6 m, and the depth of the bottom plate of the cylindrical wall seat in the frozen section is 767 m (with the wellhead as the elevation), among which the viscous soil layer accounts for 89.47%. The shaft freezing wall design principle is as follows: the Domke formula is used to calculate the frozen wall thickness of the controlled horizon in the sandy soil layer, the Vyalov–Zaretsky formula is used to calculate the frozen wall thickness of the controlled layer of viscous soil, and to calculate the height of the excavation section of the controlled horizon of the cohesive soil layer, and the "Chengbing" formula is used to calculate the average temperature

Table 3: Calculation results of the frozen wall thickness in the controlled horizon of the cohesive soil layer in west air shaft of Zhaogu No. 2 Mine.

No.	Items	Unit	Controlled layer freezing wall design parameters and freezing wall thickness calculation							
1	Layer	-	Clay		Clay		Clay			
2	Depth	m	425		535		608			
3	Depth pressure	MPa	5.473		6.903		7.904			
4	Well temperature	˚C	−6		−8		−10			
5	Average temperature of frozen wall	˚C	−16		−17		−18			
6	Freezing condition coefficient	-	1.5		1.4		1.3			
7	Calculated frozen soil strength	MPa	4.9	4.2	5.3	4.5	5.5		4.7	
8	Template height	m	4.0	4.0	4.0	4.0	4.0	3.0	4.0	3.0
9	Blasting excavation height	m	6.5	6.5	5.1	5.1	5.1	5.1	6.5	6.5
10	Calculated frozen wall thickness with h_b	m	9.5	11.7	8.6	12.1	8.7	11.0	9.5	11.7
11	Calculated frozen wall thickness with h_w	m	5.8	7.2	5.0	7.1	5.1	6.6	5.8	7.2

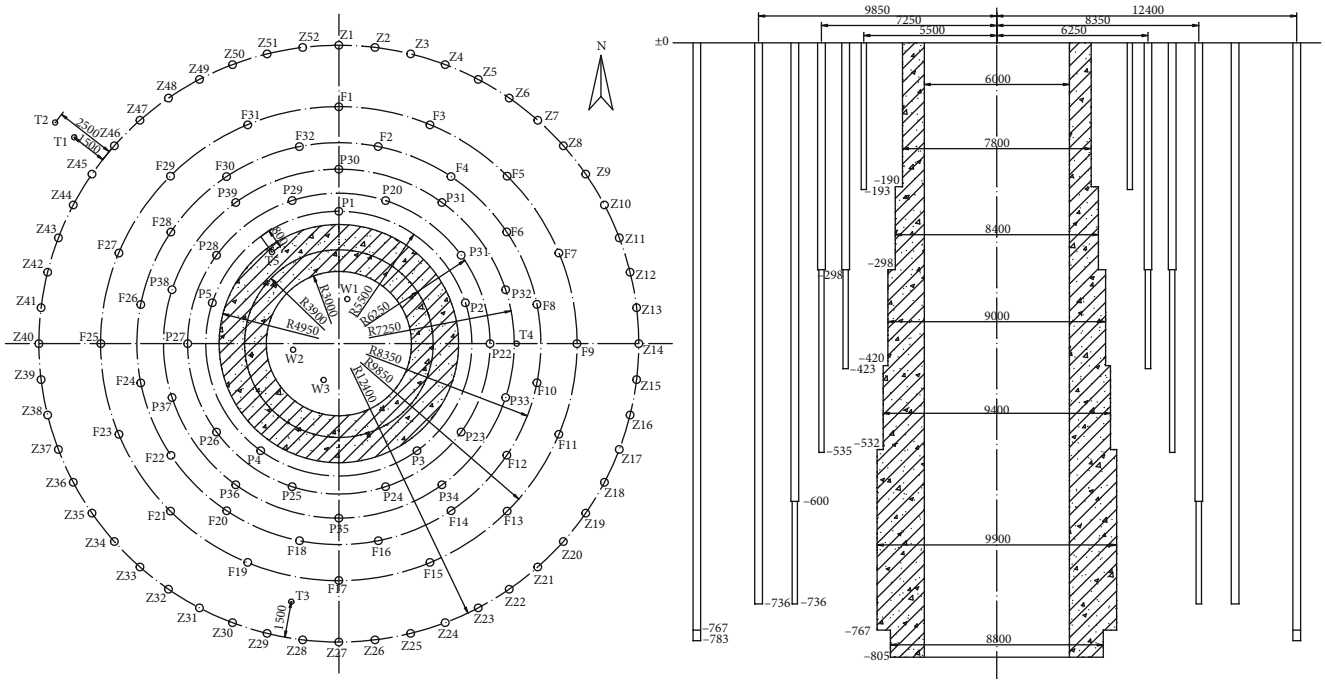

Figure 5: Layout of frozen boreholes in the west air shaft of Zhaogu No. 2 Mine.

at the effective thickness of the frozen wall. Since all the tests in this study were conducted on cohesive soil, the frozen wall thickness of the sandy soil section was no longer checked, and only the frozen wall thickness of the cohesive soil section was calculated.

Based on the analysis of alluvial burial conditions, the soil composition characteristics and shaft wall structure of the inspection hole in the west air shaft of Zhaogu No. 2 Mine, clay layers of −425, −535, and −608 m were selected as the controlled horizon of the viscous soil layer (the 4th horizon was not included because it differed significantly from the sampling depth reported in this paper). The borehole temperatures of the corresponding control layer were −6.0, −8.0, and −10.0˚C, respectively.

According to the frozen wall thickness calculation formula (1) derived from the finite length plastic thick-wall cylinder model and the fourth strength theory by Vyalov–Zaretsky formula, it is better to calculate the frozen wall thickness of the control layer of the deep alluvial cohesive soil layer under the condition of limiting the excavation section height.

$$E = \frac{\eta \cdot P \cdot h}{K}. \tag{1}$$

Here, E is the frozen wall thickness, m; P is the calculated horizontal ground pressure, MPa, according to the heavy liquid formula; h is the height of the driving section, m; K is the

Table 4: Results of the frozen wall thickness calculated according to the in situ frozen soil parameters in the control layer of the west air shaft of Zhaogu No. 2 Mine.

No.	Items	Unit	Control layer freezing wall design parameters and freezing wall thickness calculations			
1	Layer	-	Clay	Clay		Clay
2	Depth	m	425	535		608
3	Depth pressure	MPa	5.525	6.955		7.904
4	Well temperature	°C	−6	−8		−10
5	Average temperature of frozen wall	°C	−16	−17		−18
6	Freezing condition coefficient	-	1.5	1.4		1.3
7	Frozen soil strength	MPa	5.734	7.042	5.214	5.734
8	Calculated strength	MPa	4.10	5.03	3.72	4.10
9	Template height	m	4.0	4.0	4.0	4.0
10	Frozen wall thickness	m	12.35	7.83	12.27	13.05
11	Blasting excavation height	m	6.5	5.1	5.1	6.5
12	Calculated frozen wall thickness with h_b	m	13.14	9.87	14.09	13.14
13	Calculated frozen wall thickness with h_w	m	8.09	5.81	8.29	8.09

calculated strength of the frozen soil in the viscous soil, MPa; η is the coefficient of the frozen state of the working face, $\sqrt{3}$ is when the driving face is in the nonfrozen state, and $\sqrt{3}/2$ is when the driving face is frozen in real time, i.e., $\eta =$ 0.865 – 1.73. For the convenience of calculation, when the expansion range of the frozen soil in the working face is divided into 0, 1/4, 2/4, 3/4, and 4/4, the η values are 1.732, 1.516, 1.299, 1.082, and 0.865.

The designer of the original scheme proposed that the calculated strength of the frozen soil in the cohesive soil layer should take the mean value of the calculated strength of the frozen soil in similar soil layers near the controlled layer to calculate the frozen wall thickness of each layer under general conditions. The lower value is used to calculate the thickness of the frozen wall in the most unfavorable condition. Carrying out the stability measurement of the frozen wall in engineering, with which value the depth of the bottom can be adjusted, the blasting excavation period would be reduced, to meet the frozen wall thickness requirements and to improve the stability of the frozen wall design methods [27]. The value of the frozen soil strength is based on the experimental results of the remolded frozen soil from the inspection hole. At the same time, for the value of the excavation section, the actual situation of reserving the bottom-sitting blasting depth in the deep wellbore excavation should be considered. The height of the blasting excavation section is substituted into Equation (1); Table 3 presents the calculation results of the frozen wall thickness. Based on the calculation results of the controlled horizons of each viscous soil layer, the frozen wall thickness of the viscous soil layer is designed to be 9.9 m. Combined with the settlement results of the frozen wall thickness of the sand layer, the frozen wall thickness of the controlled horizon of the sandy soil layer is designed to be 10.3 m. Accordingly, Figure 5 shows the freezing hole layout.

Z_1–Z_{52} is the main freezing hole, with a ring diameter of 24.8 m and a depth of 783/767 m. The single number is the deep hole, and the double number is the shallow hole. F_1 –F_{32} are auxiliary freezing holes with a ring diameter of 19.7/16.7 m and a depth of 736 m. $P_{1\text{-}1}$–$P_{1\text{-}5}$ are small ring antislice freezing holes, with a ring diameter of 11 m and a depth of 193 m. $P_{2\text{-}1}$–$P_{2\text{-}10}$ are the freezing holes of the middle ring, with a diameter of 12.5 m and a depth of 423 m. $P_{3\text{-}1}$ –$P_{3\text{-}10}$ are large ring antislice freezing holes, with a ring diameter of 14.5 m and a depth of 535 m. T_1–T_5 are temperature measuring holes with depths of 783, 783, 535, 535, and 190 m, respectively. W_1, W_2, and W_3 are hydrological holes with depths of 210, 446, and 605 m, respectively.

4.2. Design and Calculation of Frozen Wall under Test Parameters. From Tables 1 and 2, the frozen soil sampling depths are 430, 485, 590, and 650 m. For comparative calculation, the frozen soil strength was determined using the interpolation method based on the frozen soil test results adjacent to the depth of the controlled layer and the average temperature of the frozen wall. The unconfined compressive strengths of the frozen soil are 5.734 MPa (−16°C), 7.042 MPa (−17°C), and 5.214 MPa (−18°C), respectively. Suppose the safety factor m_0 (=1.4) is the same as that in the original design, the compressive strengths of the frozen soil are 4.10, 5.03, and 3.72 MPa, respectively. According to Equation (1), Table 4 presents the calculated thickness of the frozen wall of the in situ wellbore.

Based on the frozen wall thickness calculated in Tables 3 and 4, under the same depth and calculation parameters, the frozen wall thickness calculated by in situ test strength of the frozen soil is approximately 1.14–1.61 times the original design value.

4.3. Calculation Difference Analysis. Based on the calculation method of the frozen wall thickness proposed in literature [27] and based on the designed freezing scheme, the designed frozen wall thickness and average temperature are accurately determined through in situ implementation,

prediction, and precise control of the frozen wall formation characteristics. The deviation between the effective thickness of the frozen wall and the designed effective thickness of the frozen wall is less than 2%. The deviation between the effective average temperature of the frozen wall and the designed effective average temperature of the frozen wall is less than 1°C. The deviation between the measured value of the borehole temperature and the designed control target is less than 2°C, which ensures a safe and quick passage through the frozen section. This proves that the calculation method for the freezing wall thickness and the design of the freezing scheme are scientific and feasible. In the design and calculation of the frozen wall thickness based on the undisturbed soil test results obtained from the wellbore, the value of the safety factor is still 1.4 as in the original design, which is evidently not scientific. Going forward, focus should be on designing the frozen wall thickness based on in situ frozen soil strength test results and on verifying the original freezing scheme in practice.

5. Conclusion

In this study, unconfined compressive strength tests were conducted on frozen soil sampled from Zhaogu No. 2 Mine under undisturbed and remolded conditions. The basic physical and mechanical parameters, such as the uniaxial compressive strength, elastic modulus, and Poisson's ratio, were obtained under undisturbed freezing conditions. The time effect of the stress–strain relationship of the samples was considered. The following conclusions can be drawn from the study results:

(1) The unconfined compressive strength test of the undisturbed frozen soil could be divided into four sections, and the test block exhibited a certain compressive strength even after compression failure

(2) The uniaxial compressive strength of the permafrost was negatively related to the sample temperature. The internal fissures in the permafrost and native structure increased the discreteness in the undisturbed frozen soil strength, and it is difficult to use the same law to describe. There is no specific law between buried depth and compressive strength of frozen soil

(3) The results showed that 31.3% of the elastic modulus of the undisturbed frozen soil was less than that of the remolded soil tests under the same condition. Generally, it is 0.5–2.1 times the elastic modulus of the remolded frozen soil. When applying the in situ frozen soil strength test results of the wellbore to design frozen wall thickness or verify the original freezing scheme, determining the value of the safety factor requires in-depth research and continuous improvement in practice

(4) The undisturbed frozen soil samples continued to exhibit water migration. If CT scanning is used to further analyze the variation characteristics of the microcracks before and after compression, the data will be more reliable

Data Availability

As part of the research content of the subject, the experimental data has not been disclosed. So there is no such content in the published literature or the submitted report, and this part of data has been included in the article.

Conflicts of Interest

Authors have no conflict of interest to declare.

References

[1] W. Ma, *Mechanics of Frozen Soil*, Science Press, 2020.

[2] J. L. Qi and W. Ma, "State-of-art of research on mechanical properties of frozen soil," *Rock and Soil Mechanics*, vol. 31, no. 1, pp. 133–143, 2010.

[3] H. A. Tretovitch, *Mechanics of Frozen Soil*, C. H. Q. Zhang and Y. L. Zhu, Eds., Science Press, Beijing, 1985, Trans.

[4] X. S. Chen and B. Z. Xu, "Research status and prospect of physical and mechanical properties of artificial frozen soil in China," in *Technology and Application of ground freezing engineering - Proceedings of China ground freezing Engineering for 40 years*, China Coal Industry Press, Beijing, 1995.

[5] J. P. Wang, W. M. Liu, and H. Wang, "Present state and development of China artificial ground freezing technology," *Mine Construction Technology*, vol. 40, no. 4, pp. 1–4, 2019.

[6] G. Z. Li, W. Gao, and F. Z. Li, "New progress of theory and technology in deep shaft sinking by artificial ground freezing method," *Mine Construction Technology*, vol. 41, no. 5, pp. 10–14, 2020.

[7] H. S. Li, H. T. Yang, C. Chang, and X. Sun, "Experimental investigation on compressive strength of frozen soil versus strain rate," *Journal of Cold Regions Engineering*, vol. 15, no. 2, pp. 125–133, 2001.

[8] L. Huo and B. Lin, "Experimental study on mechanical Parameters of artificial frozen clay by remolding," *Coal Engineering*, vol. 10, pp. 110–112, 2011.

[9] X. S. Chen, "Experimental study on instantaneous unconfined compressive strength of artificial frozen soil," *Well Construction Technology*, vol. 6, pp. 32–35, 1991.

[10] Z. Z. Yin, Y. L. Chen, and P. Wang, "Experimental study on uniaxial unconfined compressive strength of artificially frozen clay in Shanghai," *Rock and Soil Mechanics*, vol. 33, no. 3, p. 788, 2012.

[11] X. Huang, D. Q. Li, F. Ming, H. Bing, and W. W. Peng, "Experimental study on uniaxial compressive and tensile strength of frozen soil," *Journal of Glaciology and Geocryology*, vol. 38, no. 5, p. 1346, 2016.

[12] Z. L. Liu, H. S. Li, and Y. L. Zhu, "A timely experimental study of uniaxial compression for frozen soil," *Rock and Soil Mechanics*, vol. 23, no. 1, pp. 12–16, 2002.

[13] A. M. Fish, "Strength of frozen soil under a combined stress state," in *Proceedings of 6th international symposium on ground freezing 1991*, pp. 135–145, The Netherlands, 1991.

[14] T. H. W. Baker, S. J. Jones, and V. R. Parameswaran, "Confined and unconfined compression tests of frozen sand," in *4th*

Canada Permafrost Conference, pp. 387–392, National Research Council of Canada, Canada, 1982.

[15] H. P. Li, C. N. Lin, J. B. Zhang, and Y. L. Zhu, "Comparative experimental study on compressive strength characteristics of undisturbed and remolded artificial frozen clay," *Chinese Journal of Rock Mechanics and Engineering*, vol. 22, pp. 2861–2864, 2003.

[16] S. H. W. Chen and B. Lin, "Contrast test on uniaxial comparison of undisturbed and remolded frozen clay," *Safety in Coal Mines*, vol. 50, no. 540, pp. 62–66, 2019.

[17] P. Yang, "A study on the differences of mechanical properties between original and undisturbed frozen clays in deep," *Journal of Glaciology and Geocryology*, vol. 18, no. 3, pp. 57–61, 1996.

[18] Z. L. Liu, X. P. Zhang, and H. S. Li, "Experimental study of uniaxial compression of clay in situ," *Rock and Soil Mechanics*, vol. 28, no. 12, pp. 2657–2660, 2007.

[19] Y. L. Zhu and Kapidl, "Triaxial compressive strength of frozen soil at constant deformation rate," in *Proceedings of the Third National Conference on Frozen Soil*, pp. 179–187, Beijing: Science Press, 1989.

[20] F. D. Haynes, *Strain Rate Effect on the Strength of Frozen Silt*, Cold Regions Research and Engineering Lab Hanover NH, 1975.

[21] L. Hongsheng, Y. Haitian, C. H. Cheng, and S. Xiutang, "The strain rate sensitivity analysis of compression strength of frozen soil," *Journal of Glaciology and Geocryology*, vol. 17, no. 1, pp. 40–48, 1995.

[22] H. S. Li and C. Chang, "Sensitivity of compressive strength of frozen soil to strain rate," *Journal of Glaciology and Geocryology*, vol. 17, no. 1, pp. 40–47, 1995.

[23] L. Hongsheng, Y. Haitian, C. H. Cheng, and S. Xiutang, "The strain rate sensitivity analysis of compression strength of frozen soil," *Journal of Glaciology and Geocryology*, vol. 1, p. 47, 1995.

[24] H. P. Li, C. N. Lin, J. B. Zhang, and Y. L. Zhu, "Uniaxial compressive strength of saturated frozen clay at constant strain rates," *Chinese Journal of Geotechnical Engineering*, vol. 26, no. 1, pp. 105–109, 2004.

[25] R. A. Bragg and O. B. Andersland, "Strain rate, temperature, and sample size effects on compression and tensile properties of frozen sand," *Engineering Geology*, vol. 18, pp. 35–46, 1981.

[26] Y. L. Zhu and D. L. Carbee, "Uniaxial compressive strength of frozen silt under constant deformation rates," *Cold Regions Science and Technology*, vol. 9, no. 1, pp. 3–15, 1984.

[27] G. Z. Li, D. C. Chen, and W. Gao, "Research on design method for thickness of freezing wall in thick alluvium over 600m," *Coal Science and Technology*, vol. 48, no. 1, pp. 150–156, 2020.